General Disclaimer

One or more of the Following Statements may affect this Document

- This document has been reproduced from the best copy furnished by the organizational source. It is being released in the interest of making available as much information as possible.

- This document may contain data, which exceeds the sheet parameters. It was furnished in this condition by the organizational source and is the best copy available.

- This document may contain tone-on-tone or color graphs, charts and/or pictures, which have been reproduced in black and white.

- This document is paginated as submitted by the original source.

- Portions of this document are not fully legible due to the historical nature of some of the material. However, it is the best reproduction available from the original submission.

FINAL REPORT

INVESTIGATION OF THE DAYTIME LUNAR ATMOSPHERE

NASA GRANT NSG 7034

PRINCIPAL INVESTIGATOR

R. RICHARD HODGES, JR.

THE UNIVERSITY OF TEXAS AT DALLAS

P. O. BOX 830688

RICHARDSON, TEXAS 75083-0688

MARCH 27, 1985

INTRODUCTION

Lunar atmosphere research has tended to center on gases with predictably large sources and on those which have been identified by Apollo experiments. An early candidate atmospheric constituent was ^{40}Ar, which was noted by Heyman and Yaniv (1970) to have a surface correlated component in returned soil samples, and an abundance in excess of what can be explained by potassium decay. The source of the excess argon was attributed to atmospheric argon ions which have been accelerated by solar wind fields and implanted in soil grains (Manka and Michel, 1970, 1971).

Prior to Apollo 11, ^{40}Ar was not expected to be an important gas on the moon. Most thoughtful predictions included volcanic gases such as CO_2, H_2O, and H_2S, as well as a solar wind supplied component consisting mainly of neon. The post Apollo view is that lunar volcanism is essentially nonexistent, that the dominant gases of lunar origin are radiogenic helium, argon and radon (Hodges, 1977a), and that solar wind helium is the major source of lunar atmosphere, albeit most of this helium is trapped in satellite orbits (Hodges, 1978). Other solar wind elements, notably hydrogen and carbon, must exist in the lunar atmosphere, while nitrogen, neon and argon from the sun are less certain constituents.

Hydrogen is an enigma because the large solar wind influx of protons is certainly escaping from the moon at essentially the inflow rate, despite the fact that no hydrogen has been identified by experimental methods. The Apollo 17 orbital UV spectrometer provided an upper bound of 10 hydrogen atoms/cc (Fastie et al., 1973) which is grossly inadequate to sustain the hydrogen escape rate. Oxides and hydrides of solar wind carbon are found in lunar soil samples, suggesting molecular formation within soil grains,

1

and supporting the hypothesis that H_2 may be the form of escaping hydrogen.

Owing to the large influx of solar wind carbon, and the lack of an adequate mechanism to continually mix the soil, transporting assimilated carbon downward, it has been proposed (Hodges, 1976) that carbon inflow and escape are in balance, similar to hydrogen and helium. A major problem with this hypothesis is the lack of experimental evidence for carbon compounds in the atmosphere. However, all pertinent data from the Apollo 17 mass spectrometer were obtained during lunar night, when these gases are presumably adsorbed on surface materials. There is tentative evidence that CH_4, CO, and CO_2 exhibit argon-like presunrise increases due to lateral flow of these gases being desorbed near the terminator (Hoffman and Hodges, 1975).

While the distributions and abundances of various carbon gases in the lunar atmosphere have not been established by measurement, there is good reason to expect that they are present, and that carbon gases dominate the bound part of daytime lunar atmosphere. All other candidate gases for which model atmospheres have been computed indicate daytime concentrations less than 10^4/cc (Hodges et al., 1974).

Early predictions of a large neon atmospheric component biased both experiments and data analyses. Data from the Apollo 16 orbital mass spectrometer (Hodges et al., 1972) and the Apollo 17 lunar surface mass spectrometer (Hodges et al., 1973) provide upper bounds on nighttime neon concentrations which, perhaps fortuitously, agree with a model atmosphere (Hodges et al., 1974). Since no good lower bounds exist, the total absence of neon at night can not be ruled out. Its virtual absence from the atmosphere would imply only that soil grains are not saturated with solar wind neon; this possibility is difficult to refute based on data from returned soil sample analyses. In lunar daytime the suprathermal ion

2

detectors (SIDE) at several Apollo sites have recorded a number of events in which the solar wind v x B field was briefly aligned to accelerate atmospheric photoions into one of the SIDE instruments. Generally these events are compatible with a neon atmosphere significantly more dense than the aforementioned models (cf. Benson and Freeman, 1976). It remains to be determined whether a carbon compound, such as CO, or perhaps light metallic ions created as the result of solar wind sputtering of the lunar surface could also have produced these events.

The only gases on the moon with realistic, positive identifications and long term data bases are helium and ^{40}Ar. It is important that maximum use be made of the available data, both to understand the exospheric behavior of argon and helium, and to understand the conspicuous absence of several other candidate lunar exosphere constituents from the data. An interesting and useful aspect of the argon and helium data is the fact that argon is adsorbed at night while helium is not. In addition helium escapes kineticly while argon does not. These extreme characteristics assure that there is an experimental basis against which to test new theories regarding lunar atmosphere dynamics and the fates of the absent species.

Recent research efforts have been directed mainly toward the synthesis of the argon adsorption and diffusion properties of lunar soil, and the use of argon-40 as an archetype in attempting to understand the migratory behavior of H_2O, mercury halide compounds, and other condensible volatiles. Subsequent discussion outlines the most recent progress, and includes some preliminary material that is now being prepared for publication.

EXOSPHERE-REGOLITH ENCOUNTER SIMULATION

A significant result of this program of research was the
determination by Monte Carlo simulation that following impact on the
regolith surface of the moon (or Mercury), free exospheric atoms migrate
vertically in the soil in a random manner that is statistically similar
to a one dimensional random walk. The similarity is that the probability
of reemergence of an atom from the regolith after n collisions with soil
grains is asymptotically proportional to $n^{-3/2}$ as n becomes large (Hodges,
1980b). Long sequences of collisions are to be expected in the regolith,
as are long sequences of "bad luck" in coin flipping games. This is
necessary to account for the continual downward diffusion of some atoms,
but it also makes the mean value of n divergent. Hence, the concept of
a mean interaction time for encounters of exospheric atoms with the
regolith is meaningless.

In Monte Carlo simulation of volatile migration on the moon
an atom is traced through a succession of random thermal-speed ballistic
trajectories. When a ballistic atom impacts the regolith surface it adsorbs
on a soil grain, where it resides for a random, temperature dependent time
interval. Following desorption the atom either emerges from the regolith or
it collides with another grain where it repeats the adsorption-desorption-
flight cycle. Collisions within the soil allow vertical wandering of the
atom and, as in a one dimensional random walk, the deeper into the soil an
atom wanders, the more collisions it must make before emergence. The
probability that an atom emerges from the soil after n collisions is roughly

$$1 - \frac{1.28}{\sqrt{n+1}} \tag{1}$$

(from an emperical fit of the data in Figure 1 of Hodges, 1980b). In the
Monte Carlo lunar exosphere simulation, a random number n at each atom-

4

regolith encounter is obtained from the inverse of expression (1)

$$n = int\{1.28/u^2\} \tag{2}$$

where the operator 'int' indicates truncation of the argument to its integer value, and u is a random number chosen uniformly from the range 0 to 1.

Assuming that the atom in question makes its initial contact with a soil grain at time t_0, its probability of desorbing at time t_1 is

$$\exp\{-\int_{t_0}^{t_1} \frac{dt}{\tau}\} \tag{3}$$

where τ is the temperature dependent mean desorption time. A random deviate of t_1 is found by equating expression 3 and a random number u_1 chosen uniformly between 0 and 1. Neglecting atom flight times between collisions with soil grains, the time interval for n adsorption-desorption events is determined by the relation

$$\int_{t_0}^{t_n} \frac{dt}{\tau} = -\sum_{i=1}^{n} \ln(u_i) = -\ln(\prod_{i=1}^{n} u_i) \tag{4}$$

where t_n is the time of emergence of the atom from the regolith. Owing to the fact that the mean value of the right hand term of (4) is n, with standard deviation of $n^{1/2}$, it is convenient to approximate that term by n when n is large.

Integration of the leftmost term of equation (4) requires specification of the temperature dependence of τ, and of the time dependence of lunar surface temperature. The former is ammenable to synthesis, as will be discussed later, but the latter is somewhat subjective.

In previous models of the exospheres of the moon and Mercury it has been assumed that radiative equilibrium on a smooth, spherical surface is adequate to specify synodic temperature variations (cf. Hodges, 1973, 1974; Curtis and Hartle, 1978). However, for condensible volatiles the strong dependence of desorption time on temperature makes the distribution of small scale thermal irregularities too important to ignore. Some high lunar surface features are illuminated, and hence heated, up to 100 km on the night side of the mean terminator. At the equator this corresponds to as much as a six hour advance of local sunrise or delay of sunset. Owing to orographic surface slopes that range up to 45°, shadows are present at local solar zenith angles greater than 45°. These shadows can delay sunrise and advance sunset up to 3.7 days at the equator, and produce continuous shade at latitudes above 45°. An equatorward tilt of a surface increases the solar heat influx. For example, the north wall of a typical fresh bowl shaped crater with walls that slope 45° (Wood and Anderson, 1978), located at a latitude of 45°N, has the same insolation as a level surface at the equator. The south wall of the same crater receives no primary radiation, but it is heated by a substantial infrared flux from surrounding sunlit surfaces (Hodges, 1980b). In addition, inhomogenieties in subsurface soil conductivity cause differences in nighttime cooling rates, producing small scale temperature differences (Schultz and Mendell, 1978) that are important in view of the exponential nature of the dependence of desorption time on temperature.

The ideal computer simulator of exospheric volatile migration would be based on a thermal model that gives the actual synodic oscillation of temperature at any point on the lunar surface. This is impractical, and

6

fortunately, unnecessary. What is absolutely needed is a procedure to generate an appropriate random set of synodic temperature oscillations at any latitude. The scheme devised to do this includes generators to represent random distributions of surface slopes, of shadows and sunlight in daytime, of the illumination of tall features on the near-night side of the terminators, and of soil conductivity. These parameters are combined in emperical formulae to produce synodic temperature oscillations.

The data on which the surface temperature synodic oscillation generator is based were obtained from a large number of calculations of the temperature oscillations at various latitudes and for a variety of snadow configurations and surface parameters. The method of soil temperature calculation outlined by Keihm and Langseth (1973) was used, but with the modifications that solar illumination was truncated by shadows, and a daytime infrared reradiation flux of 12% of the local insolation was adopted from the crater temperature calculations of Hodges (1980b) to account for infrared heating of shaded areas in daytime. This resulted in a set of emperical formulae for temperature based on the variable parameters of the calculations. In the exosphere simulator, latitude is fixed by impact point, while the impact velocity vector direction sets bounds on the local slope of the soil. Longitudinal extents of insolation are determined randomly from shadow distributions based on the work of Watson et al. (1961) and Arnold (1979), and a surface slope distribution with a 6° mean slope and 45° maximum. The nighttime cooling rate is chosen randomly from a distribution that causes the model to fit the Apollo 17 orbital measurements of small scale nighttime surface temperature irregularities reported by Schultz and Mendell (1978). The complete description of the computation scheme and the emperical formulae used in the

7

exosphere simulator are found in the report entitled 'A Lunar Surface Temperature Model for Monte Carlo Exosphere Simulation.'

A key problem with the new lunar surface temperature model is that it fails to represent seasonal effects in shaded areas near the poles. In the model, latitude is measured with respect to an apparent axis that is actually the intersection of the plane of the geometric terminator and the plane of the subsolar selenographic meridian. The angle between the apparent and true polar axes varies sinusoidally with annual period and amplitude equal to the tilt of the lunar axis, or 1.53°. At low latitudes this difference is unimportant, but at 85° it causes a $\pm$ 20% variation in the lengths of day and night, and above 87° apparent latitude the model is only reasonable at the equinoxes. Owing to the small fraction of lunar surface area involved it is convenient to give the polar regions ad hoc treatment. What has proved adequate is to ignore differences between the apparent and true lunar axes at latitudes below 87°, and to assign a trapping time distribution to the polar cap regions.

Cold traps present another enigma. In Hodges (1980b) it was shown that there are permanently shaded areas that are cold enough to retain adsorbed argon for long periods, provided the soil grain surfaces in the traps are pristine. The work of Arnold (1979) and of Hodges (1981c) suggest that water contamination of the traps is unavoidable, making long term retention of argon unlikely. An important question that remains unanswered is whether the summer polar cap area is completely cleansed of adsorbed water and other volatiles, so that in winter it can provide temporary traps for argon.

INTERACTION OF ARGON ATOMS WITH LUNAR REGOLITH

One of the most impressive indicators of the pristine nature of lunar soil is the adsorption of exospheric argon-40 at night. Figure 1 shows the ^{40}Ar concentration as a function of time through two lunations at the Apollo 17 site. The data are roughly restricted to sunset to sunrise intervals, while the daytime extrapolations are results of an exospheric simulation calculation. It can be noted that just past sunset the gas concentrations begin to decrease, reaching a minimum shortly before sunrise. This decrease is caused by an excess of adsorption over desorption as the lunar surface cools. In the absence of adsorption the concentration would have increased at night, varying roughly as the -5/2 power of surface temperature (Hodges and Johnson, 1968). Sudden desorption of argon at sunrise causes a flux of gas back into night, producing the rapid increase in concentration just before sunrise.

Another important feature of Figure 1 is the distinct decrease in the amount of ^{40}Ar on the moon between March and July, 1973. This decrease requires a time varying rate of supply of argon, a phenomenon that seems out of character for the otherwise quiescent moon. Speculation on the mechanism for sporadic argon releases has ranged from a deep source in a semi-molten, core-free asthenosphere of primative lunar material (Hodges and Hoffman, 1974 and 1975; Hodges, 1977a) to near surface mylonization of crustal rock by thrust faulting (Binder, 1980), and thence to sudden desorption of argon from polar cap cold traps due to seasonal changes in shadowing (Hodges, 1980b).

Recent efforts have been directed toward an improved understanding of the interaction of exospheric ^{40}Ar with lunar regolith. Initial analyses of the Apollo 17 mass spectrometer measurements of argon resulted in
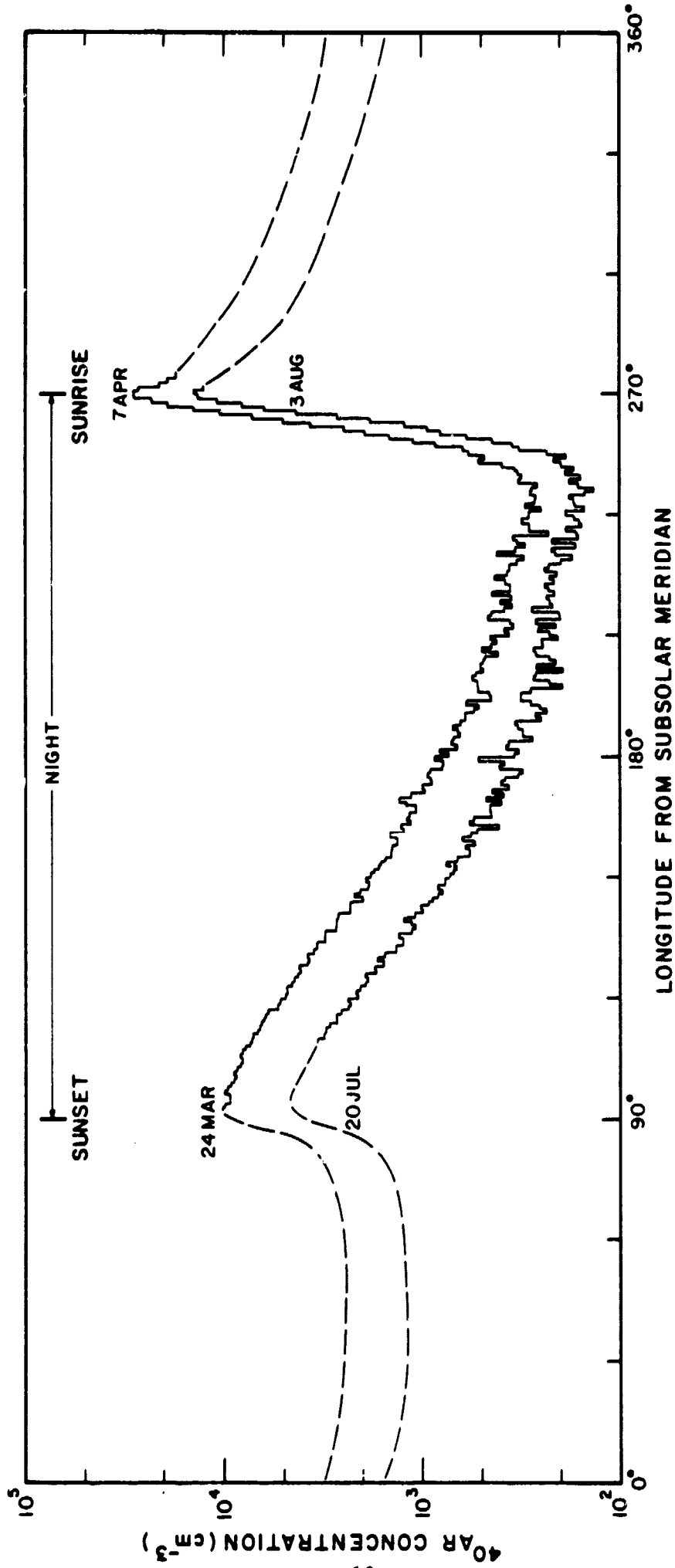
9

Figure 1. Synodic variations of ^{40}Ar measured at the Apollo 17 site during two lunations of 1973. Dashed curves are theoretical extrapolations which show the steady state daytime fluctuations.

synthesized adsorption and a minimum sticking time, which are now

recognized as mathematical artifices that approximately describe the

multiple adsorption random walk of exospheric atoms into and back out

of the soil (Hodges, 1980b).

As the argon-regolith process has become better understood,

the estimate of the activation energy for adsorbed argon has increased

from 3000 cal/mole (Hodges, 1977a) to 6000 cal/mole (Hodges, 1980b), and

subsequent discussion will show that the true value may be as large as

9000 cal/mole. The activation energy for argon on glass is about 3800

cal/mole (de Boer, 1968). The high activation energy on the moon seems

to be a verification of an intuitively attractive hypothesis, that the

degree of cleanliness of soil grains on the lunar surface is unattainable

in the laboratory, and that laboratory activation energy data necessarily

depict properties of surfaces contaminated with water vapor and possibly

other volatiles. This idea seems to be supported by the extremely low

argon activation energy (500-700 cal/mole) deduced by Frisillo et al.

(1974) from measurements of BET "C" constants for returned lunar soils

reported by Holmes et al. (1973). However, the BET "C" constants usually

give low heats of adsorption because they are determined by the last part

of monolayer formation, which occurs at sites where activation energies

are low (Holmes et al., 1973, and Frisillo et al., 1974). Thus the low

heats of adsorption of argon deduced from "C" constants may not be analogous

to the adsorption of argon on clean rocks on the lunar surface. The

difference between laboratory results for argon adsorption on glass and

on returned lunar samples is more puzzling.

The numerical value of the activation energy is greatly influenced

by the underlying assumption of functional dependence of desorption time

11

on temperature. Frisillo et al. [1974] suggested that desorpiton time should be represented by

$$\tau = \tau_o \, e^{E/RT} \qquad (5)$$

where E is the activation energy and τ_o is a constant having an expected value of 1.6×10^{-13} s. This expression was adopted by Hodges (1980b), resulting in the estimate that E = 6000 cal/mole for argon on lunar regolith.

With the implementation of the more realistic surface temperature model discussed above, it became apparent that for a constant value of τ_o, equation (5) could not represent adsorption phenomena throughout the lunar night. The quantum mechanical theory cf vapor pressure (cf. Kennard, 1938) suggests that at low temperatures τ_o must vary as T^{-2}, and hence that

$$\tau = \frac{C}{T^2} \, e^{E/RT} \qquad (6)$$

is a candidate representation of desorption time. The important difference between equations (5) and (6) in the argon exosphere simulator is that (6) decreases more rapidly than (5) as temperature increases.

Figure 2 illustrates the cype of data now emerging from the exosphere simulator calculations. The abscissa is longitude from the sub-solar meridian, but it can also be interpreted as sun hour angle at a fixed point on the rotating moon. In the lower frame the histogram shows the computed average flux of argon-40 to the regolith surface at latitudes less than 30°. A line graph superimposed on the nighttime p rt of the plot represents smoothed flux data from the Apollo 17 mass spectrometeı. The upper frame shows the average surface concentration of adsorbed argon, obtained by integration of the difference between downcoming and upgoing fluxes at the regolith surface. Following sunset, the delayed rise in adsorbed argon reflects the slow cooling of the surface, but eventually
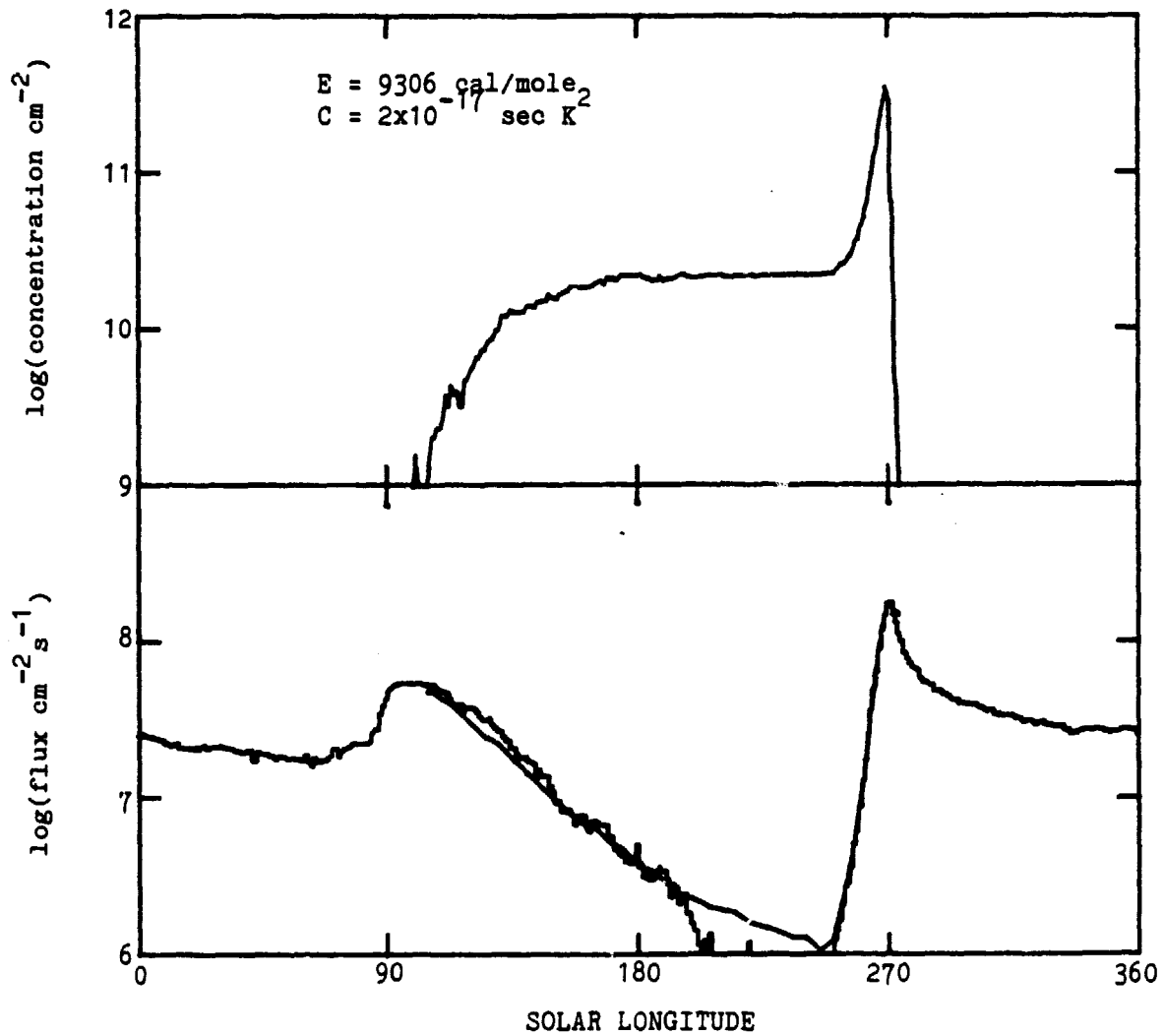
Figure 2. The downward flux of exospheric argon and the surface concentration of adsorbed argon as functions of longitude measured from the subsolar meridian.

a dominance of advection over ballistic transport causes the adsorbed argon concentration to become nearly constant. The sharp peaks at the sunrise terminator, in both the flux and the adsorbed concentration data, result from the very high probability that atoms released from the soil at the terminator will, in the course of subsequent ballistic flights, recycle to the night side of the terminator and be readsorbed.

In the simulation that produced Figure 2 the cold traps were assumed to be contaminated by water vapor and/or other frozen volatiles, making argon desorption very fast, and the traps ineffective. However, other models, with varying trap conditions, have resulted in similar reproductions of the mass spectrometer flux measurements, and in each case the surface concentration of adsorbed argon approximately duplicated the data shown in the upper part of Figure 2.

For the rapid presunrise increase in the ^{40}Ar flux to be reproduced by the simulator it is necessary that at the average presunrise surface temperature of 92K the desorption time be approximately 36 seconds. This requirement fixes the relationship of the parameters C and E in equation (6). For the exosphere simulation of Figure 2, the values $C = 2 \times 10^{-17}$ sK^2 and $E = 9306$ cal/mole were used. Models with larger values of C tend to give lower fluxes following sunset, but a change of C by several orders of magnitude is necessary to change the post-sunset flux by a factor of two.

An important descrepancy between model and experimental results occurs at the post-midnight minimum of the flux. Here the model gives essentially zero because, in the course of a succession of nighttime impact events, it is highly probable that a regolith encounter will occur wherein equation (2) generates a very large deviate for the number of adsorptions.

14

When this happens the atom is retained on the surface until sunrise. The near void in the model flux just after midnight indicates that almost all atoms suffer this fate.

The reason for the post-midnight difference between model and experimental flux data is probably due to oversin›lification in the model of the interaction process for atoms that make many adsorption collisions. To avoid rapid return to the exosphere these atoms must penetrate to depths equivalent to a large number of mean grain diameters. At night the very poor conductivity of the upper layer of soil produces a large temperature gradient (Keihm and Langseth, 1973), substantially decreasing the desorption time for exospheric atoms that penetrate to a depth of the order of one millimeter, corresponding to several hundred free path lengths. To account for this effect in an approximate way, equation (2) has been replaced by

$$n = \text{int} \left(\frac{1.28(1+K)}{u^2 + K\sqrt{u}} \right) \tag{7}$$

where K is a small number of the order of 10^{-4}. For values of $u \gg K^{2/3}$ the statistical behavior of n given by equations (2) and (7) are essentially identical, but with decreasing u the rate of growth of equation (7) becomes much slower than for equation (2). Because of the asymptotic treatment of large values of n in evaluating the right hand side of equation (4), the effect of using equation (7) to generate random values of n is equivalent to decreasing the mean desorption time for atoms that penetrate deeply into the soil.

When equation (7) is used to generate random deviates of the effective number of collisions of atoms with soil grains the expected result occurs: the argon flux throughout the nighttime decay is generally increased

15

due to desorption of atoms that previously would have been retained

until sunrise. To fit the model to the mass spectrometer measurements it

is obviously necessary to decrease E and increase C from their previously

cited values that were appropriate when equation (2) was used to determine

n. This is gratifying because a much larger value of C is also determined

from the quantum mechanical theory of vapor pressures, i.e.

$$C = \frac{h^3 e^{-5/2}}{2\pi m\sigma k^2} = 2.3 \times 10^{-12} \tag{8}$$

where h is Planck's constant, k is Boltzmann's constant, m is atomic mass,

and σ is the effective area of an adsorbed atom. Figure 3 shows model flux

and surface concentration as functions of solar longitude for $K = 10^{-4}$,

$E = 7208$ cal/mole, and $C = 2 \times 10^{-12}$ s K^2. It must be noted that this

result is based on an artificial treatment of the temperature gradient in

the soil, and that there is no present physical justification of the form

of equation (7). This is an important subject for further research because

it is pertinent to all phases of volatile migration on the moon. Questions

raised by the temporal changes in exospheric ^{40}Ar abundance on the moon, as

illustrated by the factor of two difference in the two lunations of data

shown in Figure 1, include whether the source of argon is episodic, and

how a rapid decay could be compatible with any recycling of implanted argon

ions (Hodges, 1977b). Pristine polar cap regions that serve as seasonal

cold traps were proposed by Hodges (1980b) as possible temporary sinks for

argon, allowing rapid decay of the exospheric abundance following a release,

and providing sudden releases of adsorbed gas from trap areas that reemerge

into sunlight with the approach of summer infrared reradiation levels.

The data of Figure 4 represent the time histories of two

impulsive releases of ^{40}Ar under differing conditions. In part A the winter

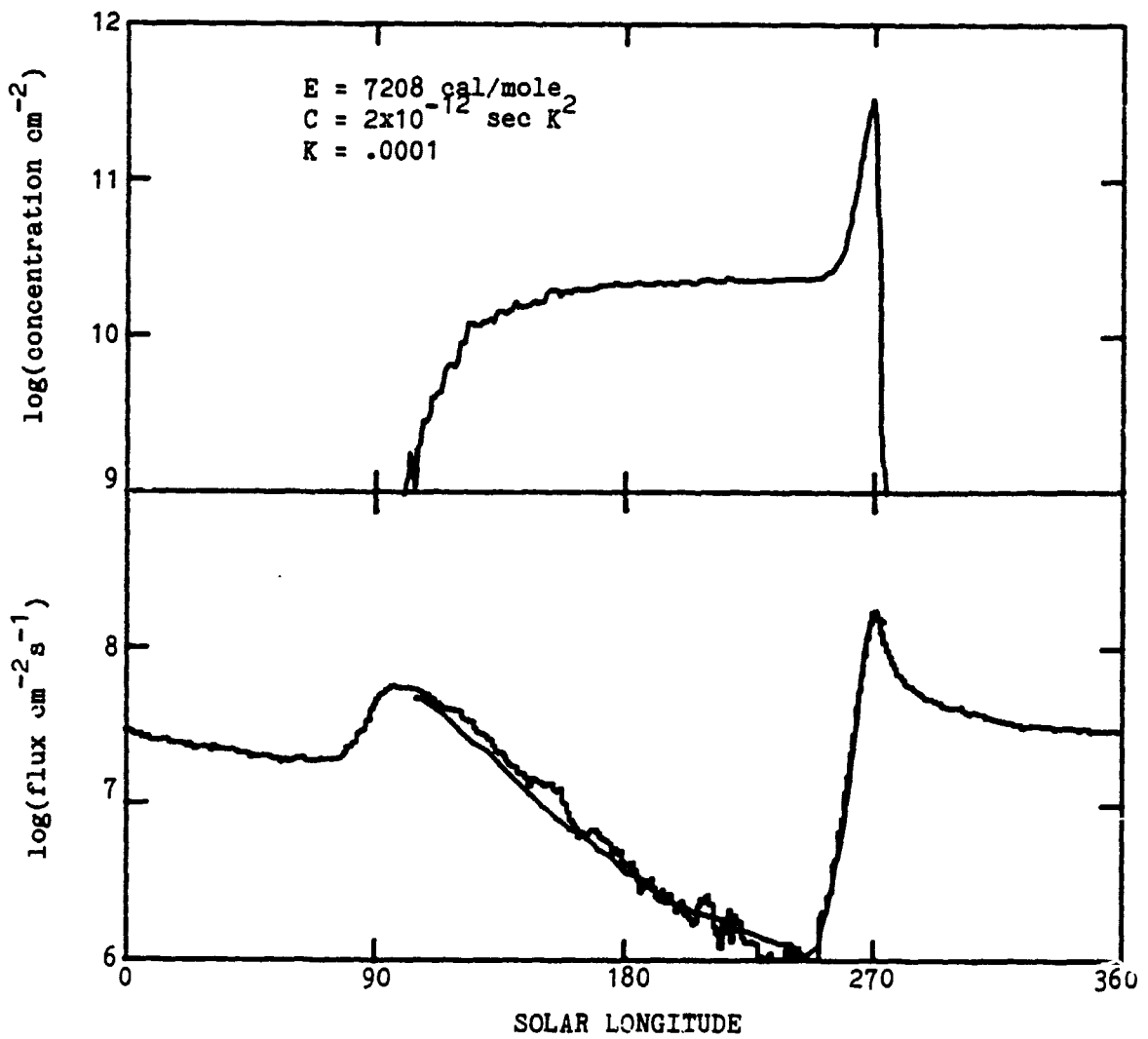polar caps were presumed to be water saturated and hence ineffective

16

Figure 3. Argon flux and surface concentration with soil temperature gradient compensation.

adsorbers of argon. Permanently shaded cold traps were assumed to be ice covered and ineffective in both cases. The sources of releases A and B were at the equatorial subsolar point. In each section of Figure 4 the diamond symbols represent the fraction of the released gas remaining on the moon as a function of time, the arithmetic difference of unity and each diamond being the fraction that has ionized. The X's denote the fraction of the release that is in the exosphere and the difference between diamonds and X's is the fraction that is adsorbed on soil grain surfaces.

Primary interest in Figure 4 centers on the exospheric fraction data (X's) because these relate to the Apollo 17 mass spectrometer measurements of argon. In case A the exospheric decay has three distinct phases, the first being a rapid decrease from unity at the time of the release to about 0.2 in less than 10 days due to adsorption on the night side. The second phase appears to last about 100 days and has a time constant of 33 days. This decay is produced by poleward migration of argon and initial capture by the winter polar cap. From 100 days on the exospheric fraction and the total argon extinction have roughly the same time constant of 2500 days. In case B the second decay phase of the exospheric fraction is missing and the third phase has a shorter time constant of 212 days.

The mass spectrometer measurements of argon-40 on the moon indicate that the main decay phase of the exospheric fraction should last. about 100 days and have a time constant that is less than 100 days. The active polar cap model, case A in Figure 4, satisfies this criterion absolutely, but the inactive polar cap model does not. In other simulations (not shown) where gas was released at high latitudes the second decay phase was also missing whether or not cold traps were active. It is not totally
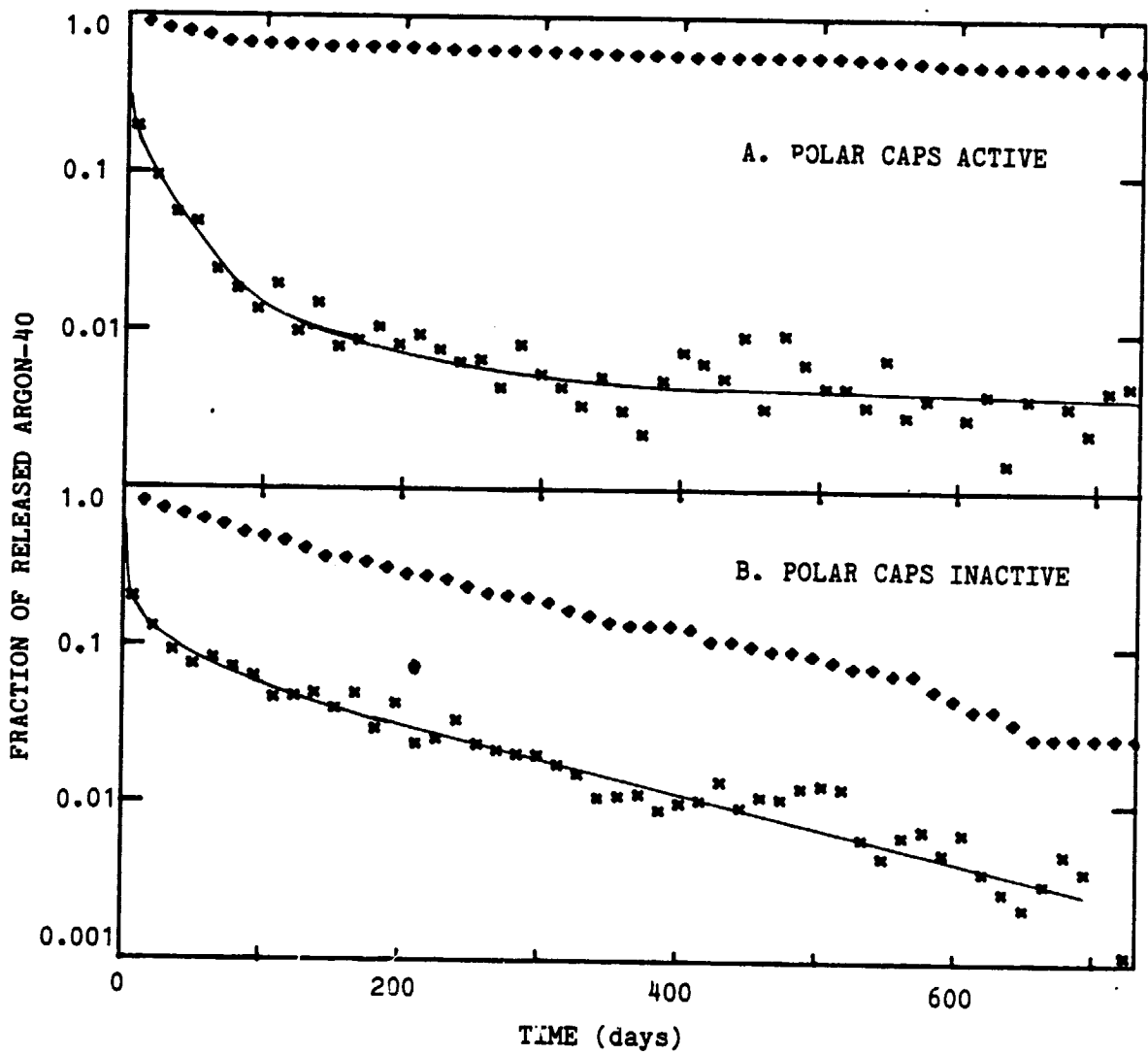
Figure 4. Time history of argon-40 released impulsively from the equatorial subsolar point. Diamonds give the fraction of the release remaining on the moon, while the X's show the fraction in the exosphere.

clear how this relates to the mass spectrometer data, but these preliminary results seem to indicate that some forms of argon cold traps exist on the moon as suggested by Hodges (1980b), and that some large argon releases occurred at low latitudes during the period of operation of the Apollo 17 mass spectrometer in 1973.

What is missing in the exosphere decay data of Figure 4 is spatial resolution. Figure 5 shows preliminary data from an exosphere model that simulates the time histories of the argon fluxes into 18 separate mass spectrometers equally spaced on the equator of the moon. Inadequate computation time is apparent in the noise that pervades this data set. However, the results are adequate to show the initial flow of argon into nighttime and the contrasting character of initial sunrises at locations that were in day and night hemispheres at the time of the gas release. Full implementation of this program is awaiting resolution of the outstanding questions discussed above regarding the soil migration and desorption processes.
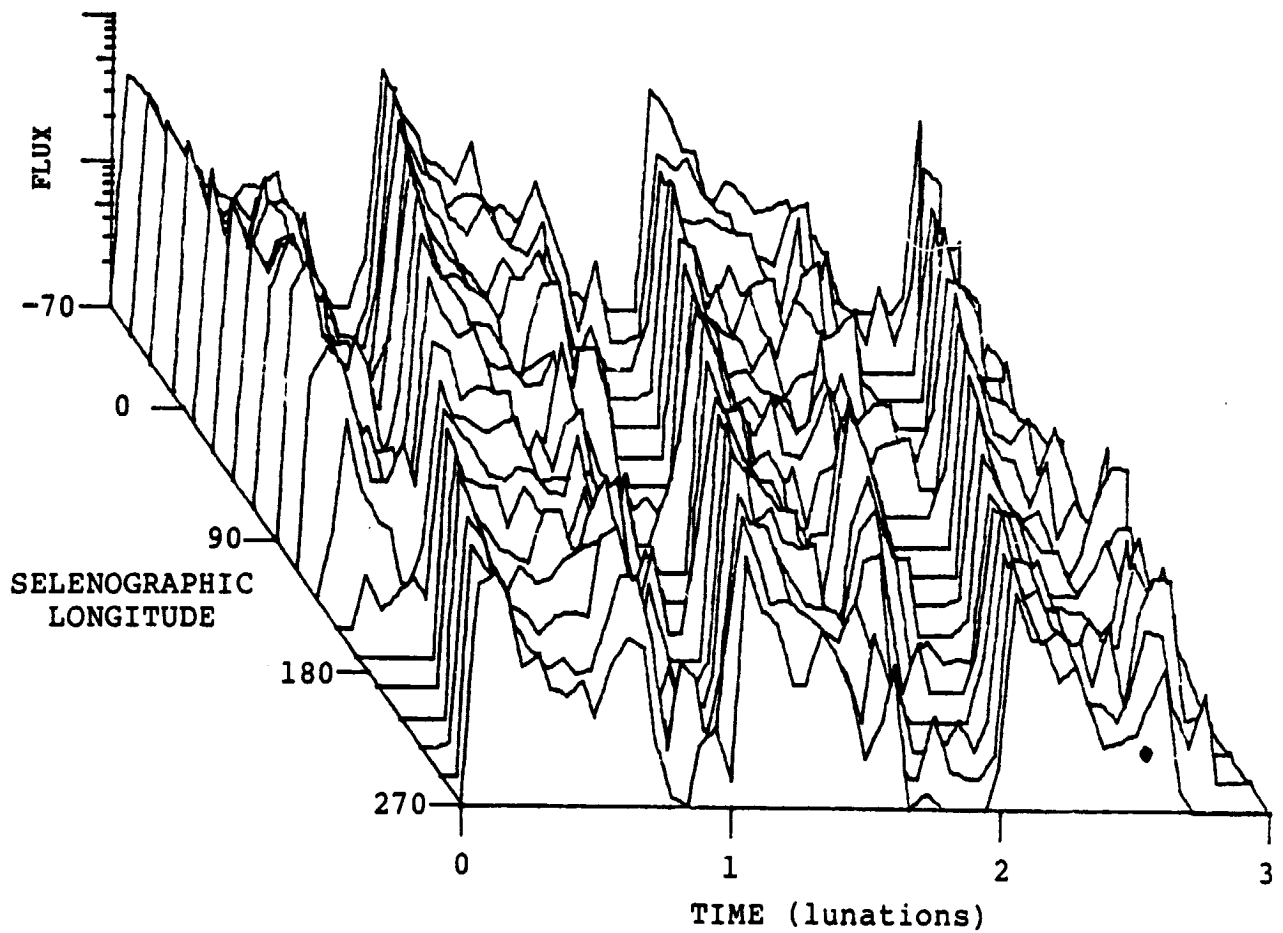
Figure 5. Argon flux at 18 equispaced points on the lunar equator following an impulsive gas release at the subsolar point at t=0.

REFERENCES

Arnold, J. R. (1979), Ice in the lunar polar regions. J. Geophys. Res., 84, 5659-5668.

Benson, J. L., and Freeman, J. W. (1976), A two-gas model of the lunar terminator exosphere, Proc. Lunar Sci. Conf. 7th, 533-541.

Binder, A. B. (1980), Shallow moonquakes: argon release mechanism, Geophys. Res. Letters, 7, 1011-1013.

Curtis, S. A., and Hartle, R.E., (1978), Mercury's helium exosphere after Mariner 10's third encounter, J. Geophys. Res., 83, 1511-1557.

de Boer, J. H., (1968), The Dynamical Character of Adsorption, 2nd ed. Oxford University Press.

Epstein, S. and Taylor, H. P., Jr. (1974), D/H and $^{18}O/^{16}O$ ratios in the rusty breccia 66095 and the origin of "lunar water", Proc. Lunar Sci. Conf. 5th, 1839-1854.

Fastie, W. G., Feldman, P. D., Henry, R. C., Mcos, H. W., Barth, C. A. Thomas, G. E., and Donahue, T. M. (1973), A search for far ultraviolet emissions from the lunar atmosphere, Science, 182, 710.

Frisillo, A. L., Winkler, J., and Strangway, D. W., (1974), Molecular flow of gases through lunar and terrestrial soils. Proc. Lunar Sci. Conf. 5th, 2963-2973.

Heyman, D., and Yaniv, A. (1970), Ar40 anomaly in lunar samples from Apollo 11, Proc. Apollo 11 Lunar Sci. Conf., 2, 1261-1267.

Hartle, R. E. and Thomas, G. E. (1974), Neutral and ion exosphere models for lunar hydrogen and helium, J. Geophys. Res., 79, 1519-1525.

Hodges, R. R. (1973), Helium and hydrogen in the lunar atmosphere, J. Geophys. Res., 78, 8055-8064.

Hodges, R. R. (1975), Formation of the lunar atmosphere, The Moon, 14, 139-157.

Hodges, R. R. (1976), The escape of solar-wind carbon from the moon, Proc. Lunar Sci. Conf. 7th, 493-500.

Hodges, R. R. (1977a), Release of radiogenic gases from the Moon, Phys. of the Earth and Planet. Interiors, 14, 282-288.

Hodges, R. R. (1977b), Formation of the lunar helium corona and atmosphere, Proc. Lunar Sci. Conf. 8th, 537-549.

Hodges, R. R. (1978), Gravitational and radiative effects on the escape of helium from the moon, Proc. Lunar Sci. Conf. 9th, 1749-1764.

Hodges, R. R. (1980a), Methods for Monte Carlo simulation of the exospheres of the moon and Mercury, J. Geophys. Res., 85, 164-170.

Hodges, R. R. (1980b), Lunar cold traps and their influence on argon-40, Proc. Lunar Planet. Sci. Conf. 11th, 2463-2477.

Hodges, R. R. (1981a), Migration of volatiles on the lunar surface, Lunar and Planet. Sci. XII, The Lunar and Planetary Institute, Houston, 451-453.

Hodges, R. R. (1981b), Exospheric transport restrictions on water ice in lunar polar cold traps, in preparation (preliminary typescript attached).

Hodges, R. R. and Johnson, F. S. (1968), Lateral transport in planetary exosphere, J. Geophys. Res., 73, 7307-7317.

Hodges, R. R., Hoffman, J. H., and Evans, D. E. (1972), Lunar Orbital Mass Spectrometer Experiment, Apollo 16 Preliminary Science Report, NASA SP-315, 21-1.

Hodges, R. R., Hoffman, J. H., Johnson, F. S., and Evans, D. E. (1973), Composition and dynamics of lunar atmosphere, Proc. Lunar Sci. Conf. 4th, 3, 2855.

Hodges, R. R., Hoffman, J. H., and Johnson, F. S. (1974), The lunar atmosphere, Icarus, 21, 415-426.

Hodges, R. R. and Hoffman, J. H. (1974a), Measurements of solar wind helium in the lunar atmosphere, Geophys. Res. Letters, 1, 69-71.

Hodges, R. R. and Hoffman, J. H. (1974b), Episodic release of ^{40}Ar from the interior of the moon, Proc. Lunar Sci. Conf. 5th, 2955-2961.

Hodges, R. R. and Hoffman, J. H. (1975), Implications of atmospheric ^{40}Ar escape on the interior structure of the moon, Proc. Lunar Sci. Conf. 6th, 3039-3047.

Hodges, R. R., Rohrbaugh, R. P. and Tinsley, B. A. (1981), The effect of the charge exchange source on the vleocity and 'temperature' distributions and their anistrophies in the earth's exosphere, J. Geophys. Res., in press.

Hodges, R. R. and Tinsley, B. A. (1981), Charge exchange in the Venus ionosphere as the source of the hot exospheric hydrogen, J. Geophys. Res., in press.

Hoffman, J. H., Hodges, R. R., and Johnson, F. S. (1973), Lunar atmospheric composition results from Apollo 17, Proc. Lunar Sci. Conf. 4th, 2865-2875.

Hoffman, J. H. and Hodges, R. R. (1975), Molecular gas species in the lunar atmosphere, The Moon, 14, 159-167.

Holmes, H. F., Fuller, E. L., Jr., and Gammage, R. B. (1973), Interaction of gases with lunar materials: Apollo 12, 14, and 16 samples, Proc. Lunar Sci. Conf. 4th, 2413-2423.

Jovanovic, S., and Reed, G. W., Jr. (1979), Regolith layering processes based on studies of low temperature volatile elements in Apollo core samples, Proc. Lunar Planet. Sci. Conf. 10th, 1425-1435.

Keihm, S. J. and Langseth, M. G. (1973), Surface brightness temperatures at the Apollo 17 heat flow site: thermal conductivity of the upper 15 cm of regolith, Proc. Lunar Sci. Conf. 4th, 2503-2513.

Kennard, E. H. (1938), Kinetic Theory of Gases, McGraw-Hill, N.J.

Manka, R. H. and Michel, F. C. (1970), Lunar atmosphere as a source of argon-40 and other lunar surface elements, Science, 169, 278-280.

Manka, R. H. and Michel, F. C. (1971), Lunar atmosphere as a source of lunar surface elements, Proc. Lunar Sci. Conf. 2nd, 1717-1728.

Reed, G. W., Jr. and Jovanovic, S. (1979), Near-surface daytime thermal conductivity in the lunar regolith, Proc. Lunar Planet. Sci. Conf. 10th, 1637-1647.

Schultz, P. H. and Mendell, W. W. (1978), Orbital infrared observations of lunar craters and possible implications for impact ejecta emplacement, Proc. Lunar Planet. Sci. Conf. 9th, 2857-2883.

Shemansky, D. E., and Broadfoot, A. L. (1977), Interaction of the surfaces of the moon and Mercury with their exospheric atmospheres, Rev. Geophys. and Space Phys., 15, 491.

Taylor, S. R. and Hodges, R. R. (1981), Chlorine and sulfur abundances in Mars and the moon: implications for bulk composition, Lunar and Planetary Science XII, The Lunar and Planetary Institute, Houston, 1082-1084.

Watson, K., Murray, B. C., and Brown, H. (1961), The behavior of volatiles on the lunar surface, J. Geophys. Res., 66, 3033.

Wood, C. A. and Anderson, L. (1978), New morphometric data on fresh lunar craters, Proc. Lunar Planet. Sci. Conf. 9th, 3669-3689.

LIST OF PUBLICATIONS

"Episodic Release of ^{40}Ar from the Interior of the Moon," with J. H. Hoffman, Proc. Lunar Sci. Conf. 5th, 3, 2955, 1974.

"Measurements of Solar Wind Helium in the Lunar Atmosphere," Geophysical Research Letters, 1, 69, 1974

"The Lunar Atmosphere," with J. H. Hoffman and F. S. Johnson, Lunar Science 5, (Lunar Science Institute, Houston), 343, 1974

"Formation of the Lunar Atmosphere," Lunar Interactions, (Lunar Science Institute, Houston), 30, 1974

"Methane and Ammonia in the Lunar Atmosphere," with J. H. Hoffman, Lunar Interactions, (Lunar Science Institute, Houston), 81, 1974

"Molecular Gas Species in the Lunar Atmosphere," with J. H. Hoffman, The Moon, 14, p. 159-167

"Episodic Release of ^{40}Ar from the Interior of the Moon," with J. H. Hoffman, Proc. Lunar Sci. Conf. 5th, 3, 2955, 1974

"Planetary Orbital Mass Spectrometry," with J. H. Hoffman, Goddard Space Flight Center Publication X-692-75-46, 25, 1975

"Implications of the Escape of Radiogenic Gases on the Internal Structure of the Moon," with J. H. Hoffman, Lunar Science 6, (Lunar Science Institute, Houston), 376, 1975

"Nonthermal Escape of Helium from the Moon," with J. H. Hoffman, Lunar Science 6, (Lunar Science Institute, Houston), 379, 1975

"Formation of the Lunar Atmosphere," The Moon, 14, p. 139-157, 1975

"Implications of Atmospheric ^{40}Ar Escape on the Interior Structure of the Moon," with J. H. Hoffman, Proc. Lunar Science Conf. 6th, 3, 3039, 1975

"The Escape of Solar Wind Carbon from the Moon," Lunar Science 7, (Lunar Science Institute, Houston) 378, 1976

"The Escape of Solar Wind Carbon from the Moon," Proc. Lunar Science Conf. 7th, 1, 493-500, 1976

"Synodic Effects on the Escape of Helium and Hydrogen from the moon," Lunar Science 8, (Lunar Science Institute, Houston), 447, 1977

"Release of Radiogenic Gases from the Moon," Phys. Earth Planet. Interiors, 14, 282, 1977

"Synodic Effects on the Escape of Helium and Hydrogen from the Moon," Lunar Science 8, (Lunar Science Institute, Houston), 447, 1977

"Formation of the Lunar Helium Corona and Atmosphere," Proc. Lunar Science Conf. 8th, 537, 1977

"Gravitational and Radiative Effects on the Thermal Escape of Gases from the Moon," Lunar and Planetary Science 9, (Lunar and Planetary Institute, Houston), 526, 1978

"Gravitational and Radiative Effects on the Escape of Helium from the Moon," Proc. Lunar Sci. Conf. 9th, 1749-1764, 1978

"Effects of Orbit Recession of the Moon on the Escape of Materials from the Lunar Surface," (abstract), in Lunar and Planetary Science X, 555-557, The Lunar Science Institute, Houston, 1979

"Methods for Monte Carlo Simulation of the Exospheres of the Moon and Mercury," J. Geophys. Res., 85, 164, 1980

"The Influence of Polar Cold Traps on Lunar Exospheric Argon-40," Lunar and Planetary Science XI, 453-455, 1980

"Lunar Cold Traps and Their Influence on Argon-40," Proc. Lunar Planet. Sci. Conf. 11th, 2463-2477, 1980.

"Migration of Volatiles on the Lunar Surface," (abstract), in Lunar and Planetary Science XII, 451-453, 1981.

"Chlorine and Sulfur Abundances in Mars and the Moon: Implications for Bulk Composition," with S. R. Taylor, in Lunar and Planetary Science XII, 1082-1084, 1981.